

Minimized atomistic model (MAM) of B_mI_n cluster

and the effect of Ge pre-amorphization implant (Ge-PAI) on boron diffusion

Jae-Hyun Yoo, Chi-Ok Hwang, Kwan-Sun Yoon, Jung-Sik Kim, and Taeyoung Won

Department of Electrical Engineering, School of Engineering, Inha University

253 Yonghyun-dong, Nam-gu, Incheon, Korea 402-751

Phone: +82-32-875-7436 Fax: +82-32-862-1350 E-mail: {yjh, twon}@hsel.inha.ac.kr

ABSTRACT

In this paper, since boron atoms tend to diffuse in the silicon crystal with complex cluster structures, KMC calculation requires an excessive CPU time during the transient stages. In this paper, we present a simplified atomistic model which includes the dominant B_mI_n clusters for fast Kinetic Monte Carlo (KMC) calculation. In this work, we propose two types of simplified atomistic models for B_mI_n clusters, which comprise a simple atomistic model (SAM) and minimized atomistic model (MAM). The proposed simplified atomistic cluster model reduces the computational burden by more than a factor of 10 even with keeping the accuracy of the full cluster model. From the investigation on the dominant B_mI_n clusters during annealing process, we could decipher the most probable process route for the evolution of clusters. Our KMC simulation revealed that B_1I_2 seems to act a dominant role at the beginning stage of annealing process while B_3I becomes more dominant near the end. After the proposed models were verified with experimental SIMS data, we implemented boron diffusion using MAM in wafer considering the Ge-PAI. The results of our simulation agreed with SIMS data.

Keywords: diffusion, Cluster modeling, Simple atomistic model, Minimized atomistic model

1 INTRODUCTION

Since CMOS channel length has shortened down to nanometer scale, it becomes more stringent to form a ultra-shallow junction in a CMOS structure. Due to the technical limit of the conventional macroscopic approach like finite element method (FEM) and finite difference method (FDM), an atomistic approach has been thoroughly investigated for the use of modeling the diffusion of impurities in silicon [1]. The KMC method is based on the Poisson process and monitors each movement of atom like migration, recombination, and hopping. However, since the KMC method requires the allocation of memory for each atom and also the computation of the transition rates of each atom for the transition to the next step, an extensive CPU time is needed. Furthermore, extracting the atomic parameters needed for KMC calculation is also a challenging task. Boron atom has a complex B_mI_n cluster structure with activated characteristic.

Our model is based on the simple continuum model, which was introduced by Charkravathi [2]. The Charkravathi's is

model was constructed by emphasizing B_1I_2 and B_3I as dominant factors for boron diffusion. We can predict the diffusion path from the calculation of the evolution energy between clusters. We also employed the interstitialcy mechanism to implement the boron diffusion in silicon. Interstitialcy mechanism describes boron atoms that combine themselves with interstitial and form mobile BI clusters and create diffusion. The Interstitialcy mechanism is the continuing diffusion process through cluster bonding and break-up phenomenon. The evolution of clusters is modeled in Eqs. 1.1 to 1.5.

$$B_s + I \leftrightarrow BI \quad (1.1)$$

$$B_mI_n + I \leftrightarrow B_mI_{n+1} \quad (1.2)$$

$$B_mI_n + V \leftrightarrow B_mI_{n-1} \quad (1.3)$$

$$B_mI_n \leftrightarrow B_mI_{n-1} + I \quad (1.4)$$

$$B_mI_n \leftrightarrow B_{m-1}I_{n-1} + BI \quad (1.5)$$

We applied our simple models to consider the Ge-PAI. The results of our simulation agreed with SIMS data.

2 SIMPLIFIED ATOMISTIC B_mI_n CLUSTER MODELS

2.1 Simple Atomistic Model (SAM)

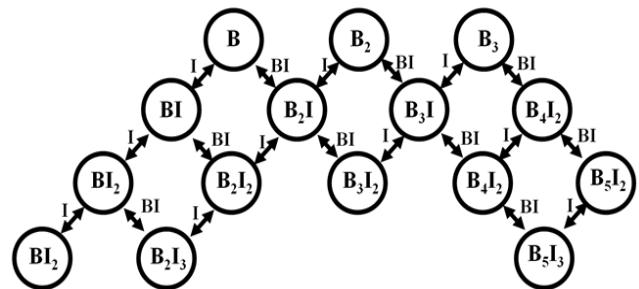


Fig. 1 A schematic diagram illustrating the conventional B_mI_n cluster structure in full atomistic model.

Figure 1 is a schematic diagram illustrating the transitional boron cluster structure in atomistic model. At the beginning of this work, we tried to use the simple continuum model, which is relatively simplified, as shown in Fig. 2. We devised a model including the simple cluster structure by assigning BI_2

and B_3I as dominant clusters as in the charkravathi's model and by allocating intermediate clusters between clusters evolution in atomic level diffusion process. However, our first trial model exhibited an unsatisfactory outcome which does not demonstrate agreement with other experimentation results.

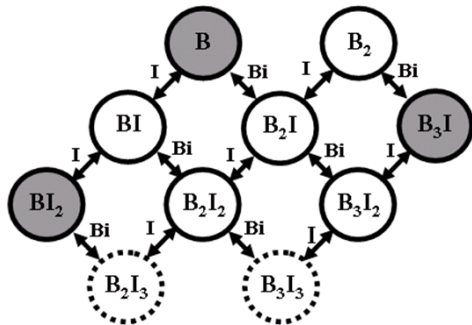


Fig. 2 A schematic diagram illustrating the simple continuum model (gray-colored) [2], our first trial model (bold line), and simple atomistic model of the prior art [3].

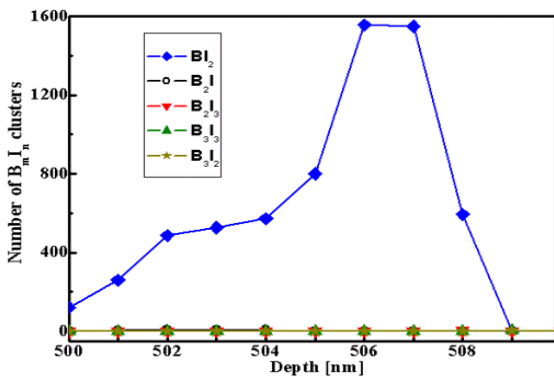
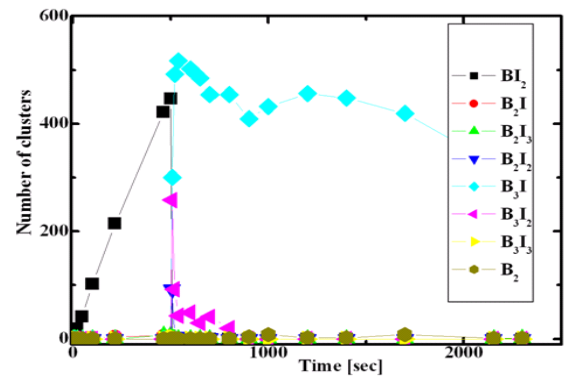


Fig. 3 A plot illustrating the evolutionary change of number of clusters as a function of time for $5 \times 10^{14} \text{ cm}^{-3}$, 20 keV boron implant, followed by a 30 min anneal at $800 \text{ }^\circ\text{C}$ between 500 and 510 seconds in the first trial model without taking B_2I_3 and B_3I_3 into account.

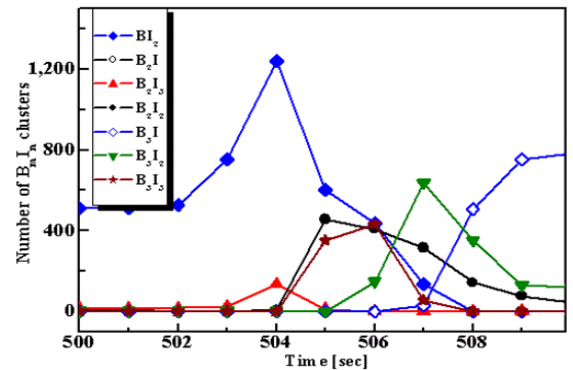
Figure 3 is a plot illustrating the change in the number of clusters when we employed our first trial model. With our first trial model, we could find out that BI_2 cluster created at the beginning of annealing process cannot evolve into B_3I that is created near the end of annealing process. Our simulation implies that there may be a medium cluster that acts an important role in helping BI_2 to evolve into B_3I so that we created a new route for them. We added several clusters in the cluster structure, and we found that B_2I_3 and B_3I_3 are the medium clusters shown as dotted line in Fig. 2. We named such cluster structure as simple atomistic model (SAM) [3].

2.2 Minimized Atomistic Model

The propose SAM model for clusters was investigated further in detail. Detailed analysis enabled us to estimate the number of clusters coming up during the annealing process shown in Fig. 5. Figure 5(b) is the simulation results with time interval of 1 second. Figure 6 is the time table of Fig. 5(b). Referring to Figures 5 and 6, we can observe that B_2 and B_2I do not occur so frequently.



(a)



(b)

Fig. 5 Plots showing the temporal change of clusters for $5 \times 10^{14} \text{ cm}^{-3}$, 20 keV boron implant, after a 30 min anneal at $800 \text{ }^\circ\text{C}$ (a) in the simple atomistic model (b) between 500 s and 510 s in the simple atomistic model.

B_2 and B_2I never showed up because the time interval in this plot was 1 second. Since it takes a few femto-seconds for an event to occur, there should be many events like cluster formation and break-ups in a second [4]. However, it seems that this repetitive phenomenon would create too much CPU time loss during the boron diffusion and that it would not interfere with boron diffusion.

Time	BI_2	B_2I	B_2I_3	B_2I_2	B_3I	B_3I_2	B_3I_3	B_2
500	513	9	17	1	1	2	1	0
501	514	9	17	1	1	2	1	0
502	528	1	18	1	1	2	1	0
503	755	1	24	1	1	2	1	0
504	1240	1	135	9	1	2	2	0
505	603	1	12	456	1	1	353	0
506	437	1	0	407	1	148	431	0
507	134	1	0	317	28	638	56	0
508	1	1	1	144	508	352	1	0
509	1	1	1	78	753	132	1	0
510	1	1	1	47	781	118	1	0
511	1	1	1	27	783	120	1	0
512	1	1	1	23	772	132	1	0
513	1	1	1	0	781	118	1	0
514	1	1	1	0	782	102	1	0
520	1	1	1	2	492	92	1	0
540	1	1	1	4	517	43	1	0
600	1	1	1	1	502	49	1	0
650	1	1	1	2	485	30	1	0
700	1	1	1	1	454	41	1	0
800	1	1	1	1	454	20	1	0
900	1	1	1	1	409	1	1	0

Fig. 6 A table showing the frequency of events occurring for each type of cluster during diffusion.

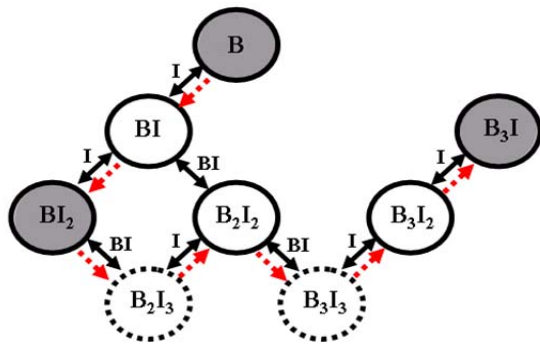


Fig. 7 A plot illustrating the minimized atomistic model (MAM) and the evolution path of dominant clusters (red dotted arrow).

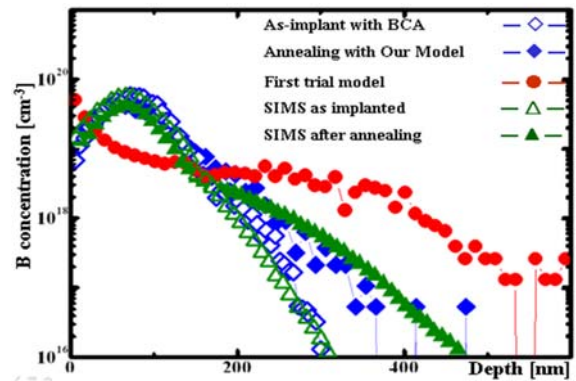
Figure 6 is a table illustrating the frequency of event occurring during the evolution for boron diffusion. The KMC calculation reveals that B_2I is the dominant cluster at the beginning while B_2I_3 and B_3I contribute much to cluster evolution when BI_2 evolves into B_3I , which becomes dominant near the end of annealing process. Figure 7 is a plot illustrating the evolution path which we found out and is indicated by arrows. This evolution path proved again that B_2I_3 and B_3I contribute to cluster evolution when BI_2 evolves into B_3I , which becomes dominant toward the end of annealing process. Consequently, we propose the minimized atomistic model (MAM), the second simplified model, as shown in Fig. 7.

3 SIMULATION RESULT AND DISCUSSIONS

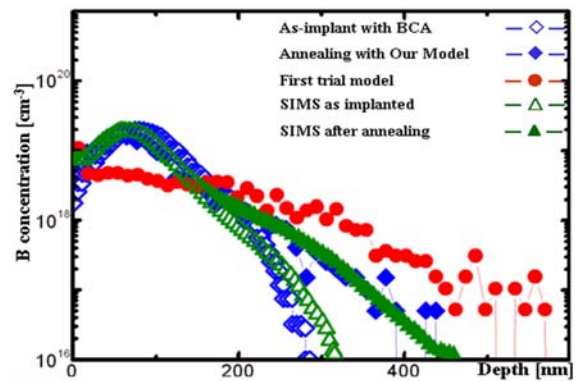
Figure 4 is a schematic diagram illustrating the simulation results when the SAM was applied. Such clusters have an important role in boron diffusion. In Figure 4 is shown the simulation results of as-implant and diffusion when the SAM and BCA were applied. The simulation was performed under the condition of boron of $5 \times 10^{14} \text{ cm}^{-2}$, 20 keV, (a) 800°C , for 2 h and (b) $2 \times 10^{14} \text{ cm}^{-2}$, 800°C , for 1 hour, respectively. These simulation results were performed based upon the above-mentioned conditions. In Figure 4, the green color-empty triangles (\triangle) depict as-implant SIMS profile, whilst the green color-filled triangles (\blacktriangle) represent SIMS profile after annealing. The blue color-empty diamonds (\diamond) indicate as-implantation using binary collision approximation (BCA), while the red color-filled circles (\bullet) show the annealing profile in first trial model after changing the simple continuum profile to the simple atomistic profile. Finally, the blue color-filled diamonds (\blacklozenge) represent the profile which we applied the simple atomistic model to through annealing process after changing the simple continuum model's atomistic clusters and adding B_2I_2 and B_3I_2 clusters. Consequently, we observed that the use of B_2I_2 and B_3I_2 enhanced the accuracy of the simulations. Referring to Figure 4, we can see that the simulation results are in good agreement with SIMS data [5, 6].

Figure 8 shows the boron profiles for different ion implantations and annealing conditions; (a) $5 \times 10^{14} \text{ cm}^{-2}$, 20 keV, followed by annealing at 800°C for 30 min, (b) 2×10^{14}

cm^{-2} , 20 keV, followed by annealing at 800°C for 1 hour for the MAM. These simulation results were performed based upon the above-mentioned conditions.



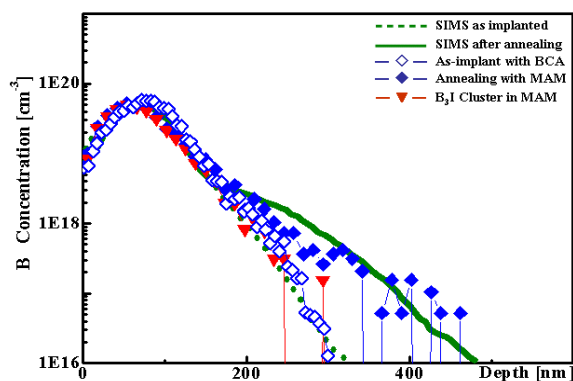
(a)



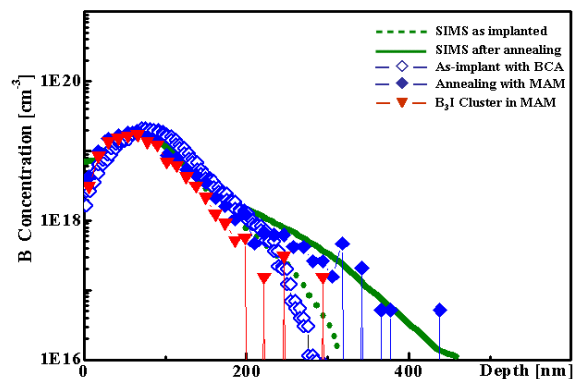
(b)

Fig. 4 Comparison of simple atomistic model to SIMS and first trial model data for boron of $5 \times 10^{14} \text{ cm}^{-2}$, 20 keV, (a) 800°C , for 2 h and (b) $2 \times 10^{14} \text{ cm}^{-2}$, 800°C , for 1 h. SIMS is obtained from M. D. Giles et al. and S. Solmi, et al., [5, 6].

In Figure 8(a), the green color-dotted line depicts as-implantation SIMS profile, while the green color-bold line represents SIMS profile after annealing. The blue color-empty diamonds (\diamond) indicate as-implant profile using binary collision approximation (BCA), while the blue color-filled diamonds (\blacklozenge) represent the profile which we applied to our MAM through annealing process. Finally, the red upside-down triangles (\blacktriangledown) indicate the profile of B_3I clusters after annealing process. Consequently, we observe that the MAM excluding B_2 and B_2I in the simple atomistic model is able to simulate the boron diffusion and B_3I plays a crucial role in boron diffusion. Here is the other simulation result under different conditions in Fig. 8 (b). As in the case of Figure 8(a), we can see the agreement between the green-colored bold lines and the blue color-filled diamonds (\blacklozenge) lines. Therefore, the dominant cluster's characteristic is proved to be very critical as intermediate clusters acting as a bridge between clusters. Also, the simulation results depicted in Fig. 8 support the reasoning that B_2I_3 and B_3I_3 play a crucial role in the evolution path of dominant clusters in boron diffusion because the evolution path consists of such intermediate clusters.



(a)



(b)

Fig. 8 Pots showing boron profiles for different ion implantations and annealing conditions; (a) $5 \times 10^{14} \text{ cm}^{-2}$, 20 keV, followed by annealing at 800 °C for 30 min, (b) $2 \times 10^{14} \text{ cm}^{-2}$, 20 keV, followed by annealing at 800 °C for 1 hour for the MAM. SIMS is obtained from M. D. Giles et al. and S. Solmi, et al., [5, 6].

Additionally, Fig. 9 illustrates the “up-hill diffusion” which reduces boron TED and minimizes the junction depth [7]. The depth with the Ge PAI is calculated to be 125 nm while the depth without the PAI is found to be 135 nm at $1 \times 10^{19} \text{ cm}^{-3}$.

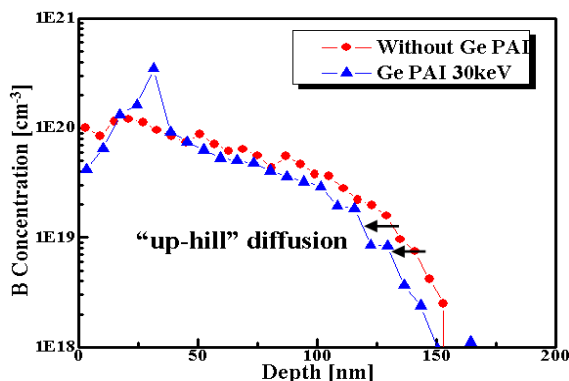


Fig. 9. Boron “up-hill” diffusion in the presence of Ge: At S/D junction, boron profiles are compared with Ge PAI wherein the implant energy is 30keV.

Figure 10 shows a good agreement between the SIMS data and the simulated curves both for samples with PAI and without PAI, respectively.

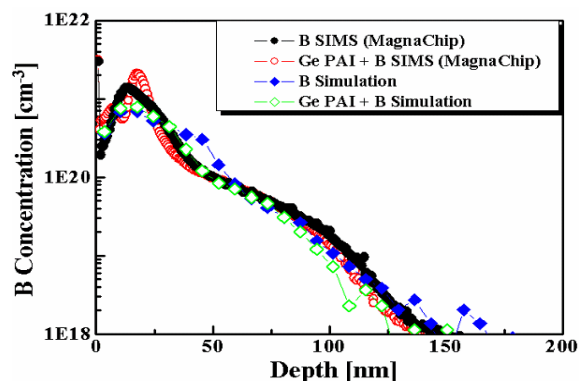


Fig. 10. Simulation results with SIMS: Ge PAI of 5 keV, $1 \times 10^{15} \text{ cm}^{-2}$, B of 3.5 keV, $3 \times 10^{15} \text{ cm}^{-2}$ and 20 keV, $2 \times 10^{13} \text{ cm}^{-2}$, annealing for 200 s at 680 °C and 10 s at 995 °C [7].

4 CONCLUSION

In conclusion, we suggested that MAM could be used for the KMC boron diffusion. We compared our simulations to experimental SIMS data. Our KMC calculations showed that B_3I is the most significant cluster in the boron diffusion posterior to annealing. We found that all kinds of intermediate clusters should be taken into account for an accurate KMC simulation and that distribution of boron in the diffusion process can be simulated with MAM. Also, we discovered the evolution path from BI_2 to B_3I in boron diffusion. In addition, using MAM, the boron diffusion in the Ge pre-amorphized silicon was simulated in the atomistic scale for the first time.

5 ACKNOWLEDGEMENT

This work was supported partly by the Korean Ministry of Information & Communication (MIC) through the Information Technology Research Center (ITRC) Program supervised by IITA, and partly by the Korean Ministry of Science and Technology (MOST) through the Tera-Nano Development (TND) Program.

REFERENCES

- [1] M. Jaraiz, G Gilmer, J. M. Poate, and T. D. Rubia, Appl. Phys. Lett., **68**, (1996), p. 409.
- [2] S. Chakravathi, And S. T. Dunham, J. Appl. Phys., **89**, (2001), p.3650.
- [3] J. H. Yoo, C. O. Hwang, J. Seo, O. S. Kwon, and T. Won, SISPAD. (2005), p.78.
- [4] K. Fichthorn, and W. H. Weinberg, J. Chem. Phys., **95**, (1991), p.1090.
- [5] SIMS data from Intel Corporation.
- [6] S. Solmi, F. Baruffaldi, and R. Canteri, J. Appl. Phys., **69**, (1991), p.2135.
- [7] N. E. B. Cowern, D. Alquier, M. Omri, A. Claverie and A. Nejim, Nucl. Instr. and Meth. In Phys. Res. B 148 (1999), p. 257.